Strong Confinement of Flexible Graphene Plasmons and Its Application

J. Wang, W. B. Lu, X. B. Li, J. Hu, and X. F. Gu
State Key Laboratory of Millimeter Waves, School of Information Science and Engineering
Southeast University, China

Abstract— The intrinsic strong confinement of flexible graphene plasmons (FGPs) is investigated in this paper, such unique property is interpreted by the ultra small thickness and metal like effective dielectric constant from the perspective of classical electromagnetic analysis. Utilizing this advantage, signals and energy can naturally propagate along curved surfaces with little curve-induced radiation loss and acceptable intrinsic propagation loss. Meanwhile, the metal plasmons (MPs) and graphene plasmons (GPs) on curved waveguides are simulated to illustrate the different property. At last, a stereo resonator is proposed as an application for the FGPs based devices.

1. INTRODUCTION

Metal plasmons (MPs), the collective oscillations of electron plasma generated by the interaction between photons and charge carriers, which can make light signals be localized and guided along the metal surfaces beyond the diffraction limit, opens the door of next generation highly compact devices [1–3]. And more specifically, when signals are expected to be manipulated at curved surfaces in many plasmonic circuits (e.g., ring resonators [4, 5]), the curve-induced radiation loss leads a considerable influence of the propagation efficiency [7–11]. Studies focusing the reduction of such radiation loss mainly include dielectric cladding [6, 12] and transformation optics [5], which greatly promotes the progress of the flexible metal plasmons (FMPs). In addition, new methods and materials are still being exploited to satisfy various application requirements, such as new property and different frequencies.

In the past few years, a new two dimensional (2D) material named graphene has been found to be able to support plasmons in the Terahertz (THz) and infrared (IR) regimes [13], which is similar with the conventional noble metals (e.g., gold and silver) in optical regime because they both exhibit a negative real part of permittivity. Graphene plasmons (GPs) are proved to be a promising alternative to the MPs with their unique tunability [13–15], which has been utilized to design reconfigurable components for various plasmonic devices. Among them, the "black hole" [16], planar lens [17, 18], four-status switch [19] and so on are proposed.

On the other hand, GPs are found to be able to confine on the curved surfaces [20] and sharp bends [21] naturally with little SIL. Therefore, such strong confinement of flexible graphene plasmons (FGPs) provides a more simple solution to adaptive plasmonic systems [22] than FMPs. In this context, this paper investigated the strong confinement of FGPs, which is by means of classical electromagnetic analysis. The lateral confinement and the propagation properties are exploited in detail. And for a better understanding of the comparison between the FMPs and FGPs, the thin metal film is discussed together with the graphene sheet.

2. THE INTRINSIC CONFINEMENT OF FGPS

2.1. The Effective Medium Model of Graphene

Compared with the complex explanation of electron behavior when the metal is irradiated by the light, the plasmonic waves can be acquired through a more simple way by using the Maxwell's equations and the boundary conditions [1]. In fact, the graphene plasmonic properties can be described through the classical electromagnetic theory which has a good agreement with the first principle calculations except its size goes down to quantum scale [23]. Here, only the bulk GPs is considered, and the graphene is modeled as an effective medium with an dielectric constant $\varepsilon_g = 1 + i\sigma/(t_g\varepsilon_0\omega)$ [24], where $t_g = 1\,\text{nm}$ is the effective thickness of single layer graphene, and the conductivity σ is calculated using the local random phase approximation (RPA) formula [25], which is related with the temperature T, Fermi level E_F, and the intrinsic relaxation time τ of carriers.

$$\sigma(\omega) = \frac{2e^2\omega_T}{\pi\hbar}\frac{i}{\omega + i\tau^{-1}}\log\left[2\cosh\left(\frac{\omega_F}{2\omega_T}\right)\right] + \frac{e^2}{4\hbar}\left[H\left(\frac{\omega}{2}\right) + i\frac{2\omega}{\pi}\int_0^\infty \frac{H\left(\frac{\omega'}{2}\right) - H\left(\frac{\omega}{2}\right)}{\omega^2 - \omega'^2}d\omega'\right] \quad (1)$$

where where $H(\omega) = \sinh(\omega/\omega_T)/[\cosh(\omega_F/\omega_T) + \cosh(\omega/\omega_T)]$, $\omega_F = E_F/\hbar$, $\omega_T = k_B/\hbar$, k_B is the Boltzmann constant and $\hbar$ is the reduced Planck constant. The first and second terms of Eq. (1) mean the intraband and interband responses respectively. Fig. 1 shows the dispersion relation of ε_g at the condition of $T = 300\,\mathrm{K}$, $E_F = 0.4$, 0.6, 0.8 eV and $\tau = 3.0e^{-13}\,\mathrm{s}$.

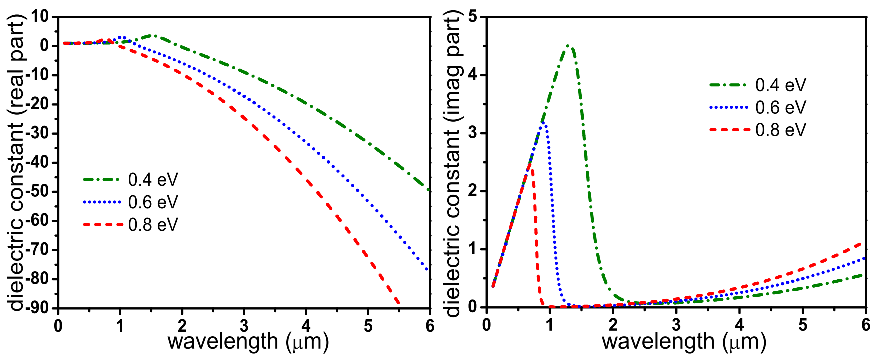

Figure 1: The dispersion relation of ε_g, (a) real part and (b) image part.

From Fig. 1, we can see that ε_g has a negative real part in the Terahertz (THz) and infrared (IR) regimes, which makes the graphene support transverse-magnetic (TM) mode waves. Moreover, on the optical regime, the the value of ε_g is positive, thus the graphene behaves a dielectric property. On the other hand, the image part of ε_g that influences the decay property of plasmonics ranges rapidly in the IR regime and slowly in THz regime, and we can find a frequency regime according to small image part of ε_g for the propagation of plasmonics at different Fermi levels.

2.2. Comparison of Graphene and Conventional Noble Metal Films

For the sake of comparison, a gold film with a finite thickness t_m and a dielectric constant ε_g calculated by the Drude model (the plasma frequency $\omega_p = 9.02\,\mathrm{eV}$ and the collision frequency $\omega_c = 0.0269\,\mathrm{eV}$) [26] is embedded in two dielectric media characterized by ε_1 and ε_2, as Fig. 2 displays.

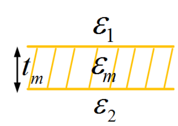

Figure 2: Gold film embedded in two media.

The characteristic equation of plasmons for the above metal film can be expressed as [27, 28]:

$$\tanh(\alpha_m t_m)(\varepsilon_1\varepsilon_2\alpha_m^2 + \varepsilon_m^2\alpha_1\alpha_2) + [\alpha_m(\varepsilon_1\alpha_2 + \varepsilon_2\alpha_1)\varepsilon_m] = 0 \tag{2}$$

where we have introduced $\alpha_j^2 = \beta^2 - \varepsilon_j k_0^2$ with $j = \{1, 2, m\}$. The transcendental set of Eq. (1) contains symmetric and antisymmetric modes, resulting two branches of the dispersion relation curves. The case of $\varepsilon_1 = 1$ and $\varepsilon_2 = 1$ corresponds to the suspended gold film, which is considered in this paper. Fig. 3 presents the normalized propagation constant with different thicknesses at 0.63 μm.

We can see from Fig. 3 that as the thickness decreases, the propagation constant divides into two modes, one is symmetric and the other is antisymmetric. It can be indicated from Fig. 3(a) that when the thickness becomes smaller, the symmetric mode plasmonic wave and free space light overlap, as a result, only the antisymmetric mode left. Simultaneously, the effective refractive index n_{eff} raises rapidly as the decrease of thickness. However, the propagation length $\ell_p = 0.5\mathrm{Im}(\beta^{-1})$ has an inverse relationship with the image part of the propagation constant, we can learn from Fig. 3(b) that the antisymmetric mode has shorter ℓ_p than symmetric mode. In short, the preliminary prediction is that the ultra thin graphene film has a large n_{eff} and a relatively small ℓ_p .

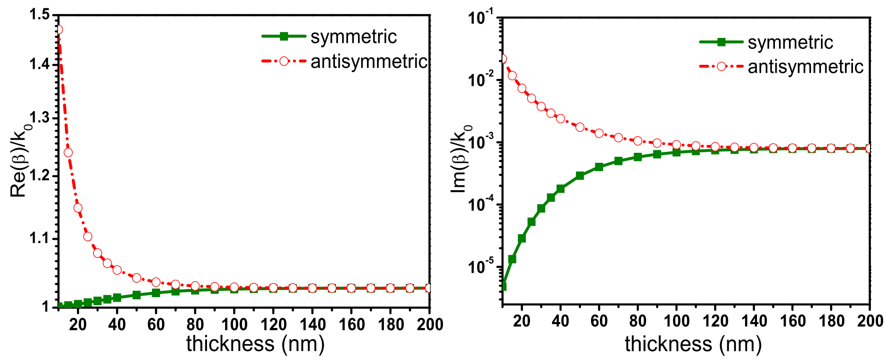

Figure 3: The relation between the (a) real part and (b) image part of the normalized propagation constant and thickness.

Next we analysis the propagation dispersion property of graphene. The propagation constant can be expressed in a simple form as [24]:

$$\beta = k_0\sqrt{1-\left(\frac{2}{\sigma\eta_0}\right)^2} \tag{3}$$

where σ is the conductivity of graphene, and η_0 is the impedance of free space. And the confinement is characterized by the lateral decay length, which is defined as $\ell = 1/\mathrm{Re}[\sqrt{\beta^2 - k_0^2}]$ [29]. Fig. 4 exhibits the propagation length (a) and lateral decay length (b) of graphene and a 40 nm gold film.

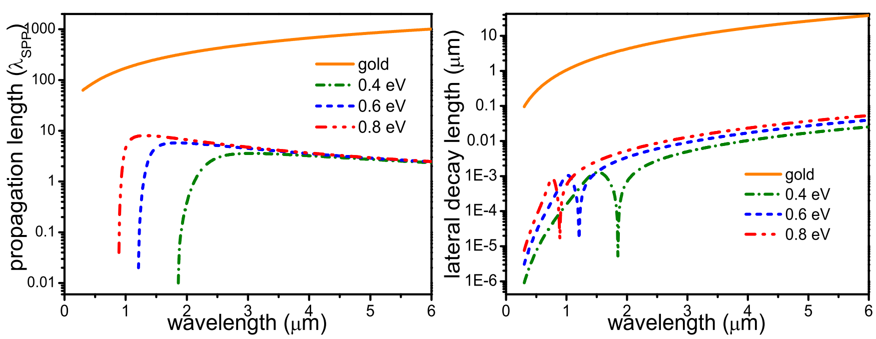

Figure 4: The (a) propagation length and (b) lateral decay length of the gold film (solid line) and the graphene (dash lines corresponding to 0.4, 0.6 and 0.8 eV).

From Fig. 4(a), we can see that the propagation length of gold film is better than graphene, and the best propagation length of graphene is approximately $8\lambda_{SPP}$, which occurs at about 1.33 µm. However, the lateral decay length of graphene is very small and times smaller than gold film, showing good confinement. Owing to the high confinement, the energy trends to propagate along bended or curved surface with little SIL.

Another parameter closely related to the confinement is the critical curvature radius for GPs. Actually, energy can be considered no longer confined when the real part of β is reduced below k_0. From this point, the critical curvature radius can be written as [20]:

$$r^* = \frac{k_0}{\mathrm{Re}[\sqrt{\beta^2 - k_0^2}](\beta - k_0)} \tag{4}$$

where we have assumed the propagation constant on the curved surface approximates to that on flat surface. With Eq. (4), the critical curvature radii in the case of 1 µm incident light for 0.8 eV doped graphene and 40nm gold film are $0.001\lambda_{SPP}$ and $95\lambda_{SPP}$ respectively, which proves further that the intrinsic confinement of graphene is better than conventional metal, and makes it easily being designed unusual shaped plasmonic devices.

3. NUMERICAL EXPERIMENT AND APPLICATION FOR FGPS

To demonstrate the difference of MPs and GPs in further, three waveguides corresponding to different curvatures are modeled, and the curve-induced radiation loss can be learned from the change of field distributions on the surface. Fig. 5 shows H_x distributions at 500 THz for 40 nm gold film based waveguide and 50 THz for graphene waveguide which is simulated by CST Microwave Studio.

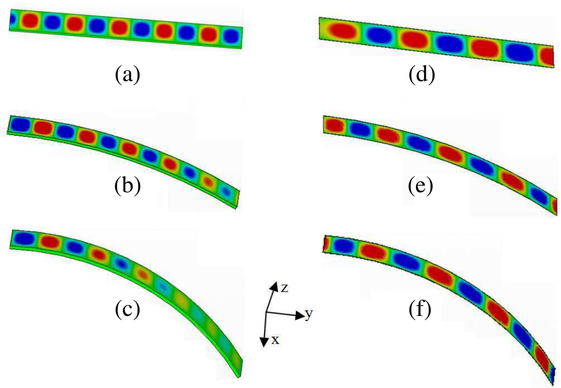

Figure 5: The propagation property of plasmonics on a)–(c) gold film (and (d)–(f) graphene waveguides corresponding to different curvatures (a), (d) infinite (the straight waveguide), (b), (e) 30 degrees, and (c), (f) 60 degrees.

From Fig. 5(a)–Fig. 5(c) we can see that few waves of MPs can propagate along the curved surface, which indicates that the MPs cannot be well supported by curved surfaces. At the same time, Fig. 5(d)–Fig. 5(f) tells us that the GPs can be well confined on curved surface.

Based on the above analysis and simulation, we increase the curvature further to 360 degrees, which forms a stereo ring resonator with the inner radius R and width W. In order to couple energy to this ring and make it work, a straight waveguide with the same width is placed near the ring, the gap between them is G, and the graphene sheet is deposited on the substrate (Al_2O_3), the scheme is illustrated as Fig. 6(a). We can see that the structure is simple and fully open (i.e., without cladding and transformation optics design).

The transmission spectrum is shown as Fig. 6(b) with the following parameters: $R = 60\,\mathrm{nm}$, $W = 40\,\mathrm{nm}$, $G = 10\,\mathrm{nm}$ and $E_F = 0.6\,\mathrm{eV}$. We can see from Fig. 6(a) that there are 3 resonances from 5 to 25 THz. What's more, the field distribution on the YOZ plane corresponding to the 3rd resonance is presented as the inset of Fig. 6(b). It can be clearly found that there are three well confined plasmonic waves on the ring, and few fields at the output, which performs as the "band-stop" function. In fact, the resonator is tunable in addition to its flexibility, the resonance mode N is the same with the number of plasmonic waves on the ring, in other words,

$$2\pi R = N\lambda_{SPP} = Nc/(f_r n_{\mathit{eff}}) \tag{5}$$

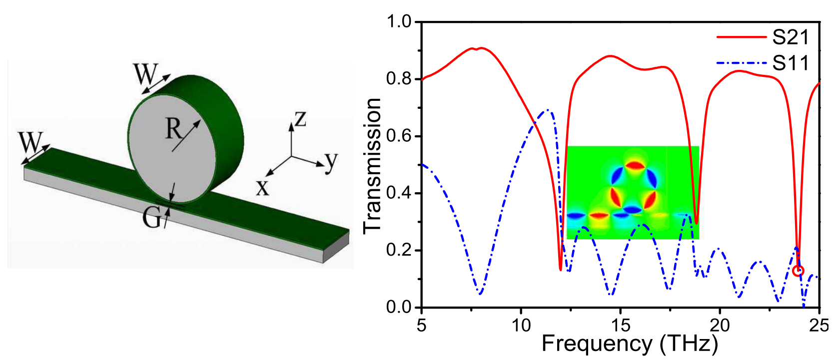

Figure 6: The scheme of the (a) stereo ring and (b) its transmission spectrum, the field distribution on YOZ plane is also provided in the inset of (b).

where c is the free space light speed, f_r is the resonance frequency. We can learn that f_r can be tuned both by the geometric size (to change R) of the ring and the doping level of graphene (to change n_{eff}).

4. CONCLUSION

In conclusion, we have investigated the FGPs from the perspective of classical electromagnetic theory. Distinguished with the conventional noble metal, the graphene can strongly confine plasmons on the surface. This feature allows us to manipulate the energy flow along the curved surface, which is proved by several demonstrations. At last, a stereo resonator is designed as the application example of FGPs. Various graphene based flexible plasmonic devices are expected to be proposed in the future.

ACKNOWLEDGMENT

This work was supported by the National Natural Science Foundation of China (Grant Nos. 61271057, 61071045), the Doctoral Fund of Ministry of Education of China (No. 20110092110009), the Fundamental Research Funds for the Central Universities and the Innovation Program for Graduate Education of Jiangsu Province (Grant No. CXLX13_092).

REFERENCES

1. Dragoman, M. and D. Dragoman, "Plasmonics: Applications to nanoscale terahertz and optical devices," *Progress in Quantum Electronics*, Vol. 32, No. 1, 1–41, 2008.
2. Gramotnev, D. K. and S. I. Bozhevolnyi, "Plasmonics beyond the diffraction limit," *Nature Photonics*, Vol. 4, No. 2, 83–91, 2010.
3. Ozbay, E., "Plasmonics: Merging photonics and electronics at nanoscale dimensions," *Science*, Vol. 311, No. 5758, 189–193, 2006.
4. Diniz, L. O., E. Marega, Jr., F. D. Nunes, and B.-H. V. Borges, "A long-range surface plasmon-polariton waveguide ring resonator as a platform for (bio) sensor applications," *Journal of Optics*, Vol. 13, No. 11, 115001, 2011.
5. Xu, H., X. Wang, T. Yu, H. Sun, and B. Zhang, "Radiation-suppressed plasmonic open resonators designed by nonmagnetic transformation optics," *Scientific Reports*, Vol. 2, 115001, 2012.
6. Berini, P. and J. Lu, "Curved long-range surface plasmon-polariton waveguides," *Optics Express*, Vol. 14, No. 11, 115001, 2011.
7. Wang, W., Q. Yang, F. Fan, H. Xu, and Z. L. Wang, "Light propagation in curved silver nanowire plasmonic waveguides," *Nano Letters*, Vol. 11, No. 4, 1603–1608, 2011.
8. Dikken, D. J., M. Spasenovic, E. Verhagen, D. van Oosten, and L. K. Kuipers, "Characterization of bending losses for curved plasmonic nanowire waveguides," *Optics Express*, Vol. 18, No. 15, 16112–16119, 2010.
9. Hasegawa, K., J. U. Nockel, and M. Deutsch, "Surface plasmon polariton propagation around bends at a metalCdielectric interface," *Applied Physics Letters*, Vol. 84, No. 11, 1835–1837, 2004.
10. Hasegawa, K., J. U. Nockel, and M. Deutsch, "Curvature-induced radiation of surface plasmon polaritons propagating around bends," *Physical Review A*, Vol. 75, No. 6, 063816, 2007.
11. Liaw, J.-W. and P.-T. Wu, "Dispersion relation of surface plasmon wave propagating along a curved metal-dielectric interface," *Optics Express*, Vol. 16, No. 7, 4945–4951, 2008.
12. Holmgaard, T., Z. Chen, S. I. Bozhevolnyi, L. Markey, A. Dereux, A. V. Krasavin, and A. V. Zayats, "Bend-and splitting loss of dielectric-loaded surface plasmon-polariton waveguides," *Optics Express*, Vol. 16, No. 18, 13585–13592, 2008.
13. Jablan, M., H. Buljan, and M. Soljacic, "Plasmonics in graphene at infrared frequencies," *Physical Review B*, Vol. 80, No. 24, 245435, 2009.
14. Ju, L., B. Geng, J. Horng, C. Girit, M. Martin, Z. Hao, H. A. Bechtel, X. Liang, A. Zettl, and Y. R. Shen, "Plasmonics in graphene at infrared frequencies," *Nature Nanotechnology*, Vol. 6, No. 10, 630-634, 2011.
15. Fei, Z., A. Rodin, G. Andreev, W. Bao, A. McLeod, M. Wagner, L. Zhang, Z. Zhao, M. Thiemens, and G. Dominguez, "Gate-tuning of graphene plasmons revealed by infrared nano-imaging," *Nature*, Vol. 487, 82–85, 2012.

16. Jiang, Y., W. B. Lu, H. J. Xu, Z. G. Dong, and T. J. Cui, "A planar electromagnetic "black hole" based on graphene," *Physics Letters A*, Vol. 376, No. 17, 1468–1471, 2012.
17. Xu, H. J., W. B. Lu, Y. Jiang, and Z. G. Dong, "Plasmonics in graphene at infrared frequencies," *Applied Physics Letters*, Vol. 100, No. 5, 051903, 2012.
18. Xu, H. J., W. Bing Lu, W. Zhu, Z. G. Dong, and T. J. Cui, "Efficient manipulation of surface plasmon polariton waves in graphene," *Applied Physics Letters*, Vol. 100, No. 24, 243110, 2012.
19. Wang, J., W. B. Lu, X. B. Li, Z. H. Ni, and T. Qiu, "Graphene plasmon guided along a nanoribbon coupled with a nanoring," *Journal of Physics D: Applied Physics*, Vol. 47, No. 13, 245435, 2014.
20. Lu, W. B., W. Zhu, H. J. Xu, Z. H. Ni, Z. G. Dong, and T. J. Cui, "Flexible transformation plasmonics using graphene," *Optics Express*, Vol. 80, No. 24, 245435, 2009.
21. Zhu, X., W. Yan, N. A. Mortensen, and S. Xiao, "Bends and splitters in graphene nanoribbon waveguides," *Optics Express*, Vol. 21, No. 3, 3486–3491, 2013.
22. Aksu, S., M. Huang, A. Artar, A. A. Yanik, S. Selvarasah, M. R. Dokmeci, and H. Altug, "Flexible plasmonics on unconventional and nonplanar substrates," *Advanced Materials*, Vol. 23, No. 38, 4422–4430, 2011.
23. Thongrattanasiri, S., A. Manjavacas, and F. J. G. de Abajo, "Quantum finite-size effects in graphene plasmons," *ACS nano*, Vol. 6, No. 2, 1766–1775, 2012.
24. Vakil, A. and N. Engheta,, "Transformation optics using graphene," *Science*, Vol. 332, No. 6035, 1291–1294, 2011.
25. Emani, N. K., T. F. Chung, X. Ni, A. V. Kildishev, Y. P. Chen, and A. Boltasseva, "Electrically tunable damping of plasmonic resonances with graphene," *Nano Letters*, Vol. 12, No. 10, 5202–5206, 2012.
26. Ordal, M., L. Long, R. Bell, S. Bell, R. Bell, R. Alexander., Jr., and C. Ward, "Optical properties of the metals Al, Co, Cu, Au, Fe, Pb, Ni, Pd, Pt, Ag, Ti, and W in the infrared and far infrared," *Applied Optics*, Vol. 22, No. 7, 1099–1119, 1983.
27. Burke, J., G. Stegeman, and T. Tamir, "Surface-polariton-like waves guided by thin, lossy metal films," *Physical Review B*, Vol. 44, No. 11, 5855, 1991.
28. Tassin, P., T. Koschny, M. Kafesaki, and C. M. Soukoulis, "A comparison of graphene, superconductors and metals as conductors for metamaterials and plasmonics," *Physical Review B*, Vol. 6, No. 4, 259–264, 2012.